Experimental and theoretical studies on C-band bismuth-based erbium doped fiber amplifier

R. PARVIZI[a], S. D. EMAMI[b], S. SHAHI[a], S. W. HARUN[a, b], H. AHMAD[a]
[a] Photonics Research Center, Department of Physics, University of Malaya 50603, Kuala Lumpur, Malaysia
[b]Department of Electrical Engineering, Faculty of Engineering, University of Malaya 50603 Kuala Lumpur Malaysia

A performance of the Bismuth-based Erbium-doped fiber amplifier (Bi-EDFA) is experimentally and theoretically investigated using 1480nm forward pumping scheme. In the theoretical analysis, the rate and power propagation equations are solved to examine the effect of fiber length on the bandwidth of the gain spectra. At C-band region, the small signal gain of the Bi-EDFA varies from 20 to 23dB with 49cm long Bi-EDF and 150mW of 1480nm pump power. It is shown that the calculated gain and noise figure are in good agreement with the experimental results, verifying the feasibility of our theoretical model. However, the experimental result shows a relatively lower gain and higher noise figure compared to the theoretical result due to the spurious reflection in the cavity and insertion loss of the Bi-EDF which were neglected in our theoretical model.

1. Introduction

Wavelength-Division Multiplexing (WDM) technologies, which allow many channels with different wavelengths to be transmitted simultaneously on a single fiber, are being used for large capacity long-haul optical transmission systems and networks. The usable spectral band for a WDM system strongly depends on the gain bandwidth of the fiber amplifiers. Since silica based transmission fibers have a wide window from 1.4–1.7 μm, amplification over all these ranges are required for broader-band WDM systems. C-band amplification from 1.53–1.56 μm was first accomplished using silica-based erbium doped fiber amplifiers (EDFAs) [1-3]. In order to extend C-band to longer wavelength range, several glass hosts such as tellurite [4], multi-component silicate [5], and bismuth oxide based glass [6] have been developed. So-called L-band amplification was realized by using a tellurite fiber in the late 1990s [7]. As a promising candidate for such wideband amplification, it has been developed Bi2O3-based Er-doped fibers (Bi-EDFs) [8]. Recently, Bismuth-based erbium-doped fibers (Bi-EDFAs) have been extensively studied for use in compact amplifiers with short gain medium lengths. This fiber incorporation quenching of the erbium ions in the fiber [9], which allows the erbium ion concentration to be increased to more than 3000 ppm.

In this paper, the amplification characteristics of the Bi-EDF are theoretically and experimentally investigated. In the theoretical study, the energy level, transition configuration, and numerical model of a Bismuth-based erbium-doped fiber amplifier are presented. With a three-level system, the rate and power propagation equations of the numerical model are solved to examine the effect of the fiber length on the bandwidth of the gain spectra. To verify the simulated results, the gain and noise figure

characteristics of the C-band Bi-EDFA is also experimentally demonstrated.

2. Experimental set up

Fig. 1 depicts the experimental setup of Bi-EDFA with a forward pumping scheme. Optical isolators are incorporated at input and output ends of the amplifier to prevent a spurious reflection from disturbing the operation of the amplifier. Wavelength division multiplexing (WDM) coupler is used to combine the pump light from 1480nm laser diode with the input signal. The Bi-EDF used in this experiment is commercially available from Asahi Glass Co and has an Er3+ ion concentration of 7.6 × 10^{25} ions/m^3 with a Lanthanum ion co-doped concentration of approximately 4.4 wt%. The fiber used has a length of 49 cm, a core/cladding refractive index of 2.03/2.02 and a NA of 0.20. It is angle spliced to a single-mode fiber in order to reduce splice point reflections.
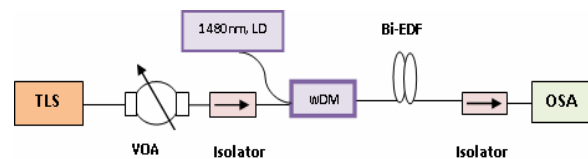

Fig. 1. Experimental set up of Bi-EDFA.

3. Numerical model

The energy level diagram of the Bi-EDF is shown in Fig. 2. The electron is excited by the pump from ground state ($^4I_{15/2}$) to excited state ($^4I_{11/2}$) and then non-radioactively transits to the meta-stable energy level

($^4I_{13/2}$). After that, it transits from the meta-stable level to the ground state with emission of 1550nm photons. Assume that the population densities of Er^{3+} ions at the $^4I_{15/2}$, $^4I_{13/2}$ and $^4I_{11/2}$ are N_1, N_2 and N_3, respectively, and the steady-state rate equations for the Bi-EDFA system can be written as:

$$\frac{dN_1}{dt} = (A_{21} + R_{S21} + R_{P21} + R_{ASE21})N_2 - (R_{S12} + R_{P12} + R_{ASE12})N_1 + C_{CUP}N_2^2 \tag{1}$$

$$\frac{dN_2}{dt} = -(A_{21} + R_{S21} + R_{P21} + R_{ASE21})N_2 + (R_{S12} + R_{P12} + R_{ASE12})N_1 - 2C_{CUP}N_2^2 + W_{32}N_3 \tag{2}$$
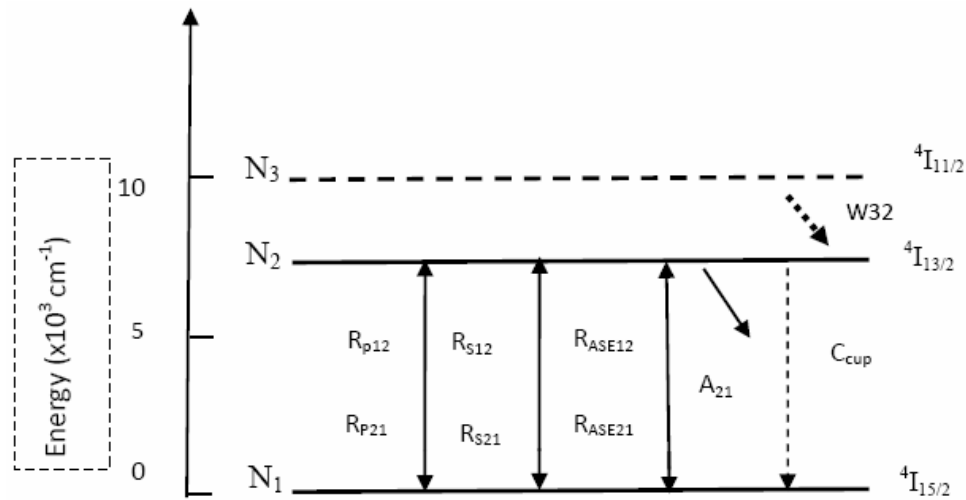
$$\frac{dN_3}{dt} = -W_{32}N_3 + C_{CUP}N_2^2 \tag{3}$$

Fig. 2. Peak energy level diagram of Er^{3+} and the relevant transitions.

where A_{21} is spontaneous emission probability of the 1.55 μm-band calculated by Fuchtbauer–Ladenburg formula, and W_{32} is non-radiative decay rate from the $^4I_{11/2}$ level that calculated by the measured lifetime [10]. ρ is total erbium ion concentration in the core of the Bi-EDF fiber. We neglected the non-radiative decay rate of the $^4I_{13/2}$ level and the spontaneous emission from the $^4I_{11/2}$ level because A_{21} and W_{32} were dominant in those levels. In steady state condition the amount of ion population doesn't change by time. C_{cup} is cooperative up conversion coefficient calculated with Snoek's method [11]. We assume that all the Er^{3+} ions excited to the $^4I_{9/2}$ levels by the cooperative up conversion process relax to the $^4I_{11/2}$ immediately. R represents the radiative decay late of the signal, pump, and ASE expressed as follows [12]:

$$\rho = N_1 + N_2 + N_3 \tag{4}$$

$$R_{S21} = \lambda_S \sigma_S^e \left(\frac{P_S}{hcA_{eff}}\right) \tag{5}$$

$$R_{S12} = \lambda_S \sigma_S^a \left(\frac{P_S}{hcA_{eff}}\right) \tag{6}$$

$$R_{P12} = \lambda_P \sigma_P^a \left(\frac{P_P}{hcA_{eff}}\right) \tag{7}$$

$$R_{P21} = \lambda_P \sigma_P^e \left(\frac{P_P}{hcA_{eff}}\right) \tag{8}$$

where h, A_{eff} and P_P are the plank constant, the effective area of the core and pump power, respectively. σ_P^e and σ_P^a are the emission and absorption cross sections at pumping wavelength, respectively while σ_S^e and σ_S^a are the emission and absorption cross sections as a function of input signals estimated from [9].

The evolution of pumps power, ASE powers and signal power along the Bi-EDF fiber (z) is given as [12];

$$\frac{dP_S}{dz} = \Gamma(\lambda_s)(\sigma_S^e N_2 - \sigma_S^a N_1) \times P_S - \alpha_S P_S \tag{9}$$

$$\frac{dP_P}{dz} = \Gamma(\lambda_P)(\sigma_P^e N_2 - \sigma_P^a N_1) \times P_P - \alpha_P P_P \tag{10}$$

$$\frac{dP_{ASE}(\lambda_{ASE})}{dz} = \Gamma(\lambda_{ASE})(\sigma_e^s N_2 - \sigma_a^s N_1) \times P_{ASE} + \Gamma(\lambda_{ASE})h\nu\Delta\nu\sigma_e^s N_2 - \alpha_{ASE}P_{ASE} \tag{11}$$

where Γ is the overlap factor of every wavelength [13] and α is the fiber background loss measured [12]. The subscripts s and ASE mean the signal and the ASE, respectively. In the ASE equation, $\Delta\nu$ represents the effective ASE bandwidth that is the resolution of the measuring device such as an optical spectrum analyzer.

4. Numerical calculation

The gain of the Bi-EDFA is calculated by solving numerically Eq. (1) - (11) above. Parameters used in the calculations 3×10^8 m/s for the light speed c in vacuum, 6.626×10^{-34} m^{2}kg/s for the Planck's constant h, 2.7×10^{-6} m for the radius of the optical fiber and 8.5×10^{-24} for the $C_{CUP.}$. The pump and input signal powers are fixed 150mW and 10^{-3}mW, respectively; and the fiber background loss is 0.6dB/m. All of equation used for pump, signal and pump power are first order differential equations. We have used P_P (z=0) = P_P, P_S (z=0) = P_S and P_{ASE} (z=0) = 0 as the boundary conditions on pump power, signal power and ASE spectral at input signal wavelength. To get accurate result a relaxation method is used by dividing fiber to many small segments of 10cm long. The noise figure of the Bi-EDFA is calculated by this equation.

$$NF = 1/G + P_{ASE}/(G \times h \times \nu \times \Delta\nu) \tag{12}$$

5. Result and discussion

Fig. 3 shows the calculated gain as a function of Bi-EDF's length at various input signal wavelength. In this calculation, the erbium ion concentration and pump power are set at 7.6×10^{25} ions/m^3 and 150mW, respectively. As shown in the figure, the maximum gains of 26dB, 20dB and 15dB are obtained for 1530, 1575 and 1615nm at Bi-EDF's length of 1.0m, 1.0 m and 1.5m respectively. At a long Bi-EDF length, the gain of the Bi-EDFA shifts to a longer wavelength region (L-band) as depicted in Fig. 3. This is attributed to the quasi two level system effects in the Bi-EDFA, which the C-band photons are absorbed to emit at a longer wavelength. Fig. 4 shows the gain and noise figure characteristics of the Bi-EDFA at the pump power of 150mW and the Bi-EDF's length of 49cm. The input signal power is fixed at -30dBm. The gains are observed in both C- and L-band region with the higher gain is obtained at the C-band region ranging from 1530 to 1560nm. It is shown that the calculated value is in good agreement with the experimental measured one, verifying the feasibility of our theoretical model.
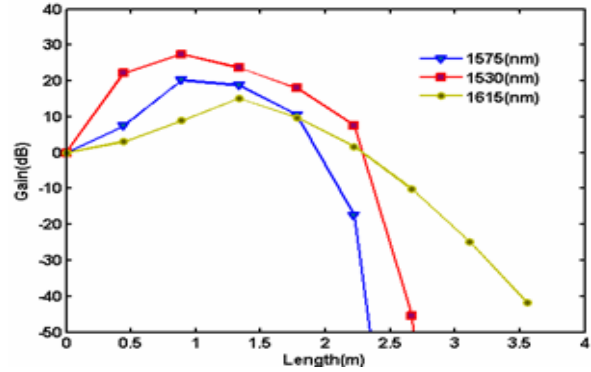

Fig. 3. Variation of gain as a function of Bi-EDF's length for three different input signal wavelengths.

The theoretical and experimental gains of the Bi-EDFA are obtained within 20 to 23dB at C-band region. The theoretical gain is flat within 35nm bandwidth from 1530nm to 1565nm as shown in Fig. 4. The slightly lower gain for the experimental results especially at longer wavelengths is expected due to the effect of multiple reflections from both the fiber splice points whereby the signal is reflected back into the Bi-EDF due to the large refractive index difference. This causes the increased cavity loss and spurious laser generation which suppresses the gain of the Bi-EDFA. As shown in Fig. 4. The Bi-EDFA gain bandwidth covers until the extended L-band region and is also much wider than that of the standard Si-EDFA. This is attributed to the suppression of excited state absorption (ESA) effect by the incorporation of La ions in the Bi-EDFA. The suppression of ESA reduces the dissipation of pump energy and increases the population inversion especially at extended L-band region. The experimental noise figure is obtained at approximately 7 dB within the C-band region as shown in Fig. 4. The high erbium ion doping concentration and high insertion loss of the Bi-EDF incur a high noise figure for the Bi-EDFA. The theoretical noise figure is lower since the insertion loss of the Bi-EDF was ignored during simulation.
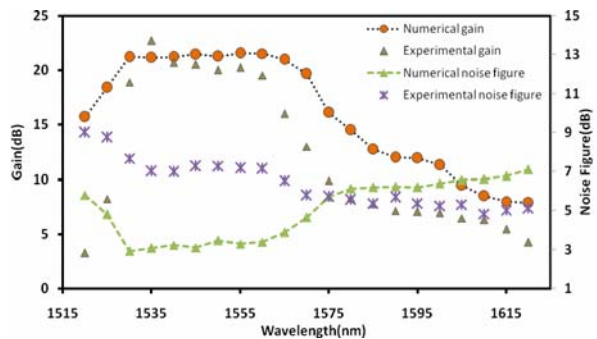

Fig. 4. Comparison of calculated gain and noise figure with experimental results for the Bi-EDFA with 49cm long Bi-EDF.

Fig. 5 shows the theoretical gain spectrum of the Bi-EDF with variation of Bi-EDF length from 0 to 1m. The input signal and pump powers are set at -30dBm and 150mW, respectively. As shown in Fig. 5, the gain of the Bi-EDFA is remarkable in C band with a shorter length of Bi-EDF and as the length increases the gain increment is more pronounced in L band region. The optimum length for the Bi-EDFA to operate in C-band is around 0.5 to 0.8m.
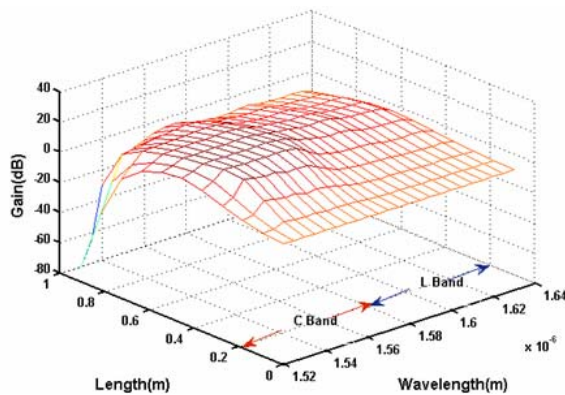

Fig. 5. Theoretical gain vs input signal wavelength and Bi-EDF's length for the Bi-EDFA.

5. Conclusions

The gain and noise figure characteristics of the Bi-EDFA have been experimentally and theoretically investigated. In the theoretical analysis, the rate and power propagation equations are solved to examine the effect of the fiber length on the bandwidth of the gain spectra. The gain of the Bi-EDFA is remarkable in C band with a shorter length of Bi-EDF and as the length increases the gain increment is more pronounced in L band region. The optimum length for the Bi-EDFA to operate in C-band is around 0.5 to 0.8m. It is shown that theoretical results are in good agreement with the experimental results, verifying the feasibility of our theoretical model.

References

[1] R. J. Mears, L. Reekie, I. M. Jauncey, D. N. Payne, Electron. Lett. **23**, 1026 (1987).
[2] F. I. Vasile, P. Schiopu, J. Optoelectron. Adv. Mater. **6**(4), 1207 (2004).
[3] I. Bibac, J. Optoelectron. Adv. Mater. **3**(1), 51 (2001).
[4] J. S. Wang, E. M. Vogel, E. Snitzer, Opt. Mat. **3**, 187 (1994).
[5] A. J. W. Ellison, J. E. Dickinson, D. E. Goforth, D. L. Harris, J. T. Kohli, J. D. Minelly, B. N. Samson, J. K. Trenteman, M. J. Yadlowsky, in proc. of Opt. Amplifiers and Their Applications, 51, 1999.
[6] S. Tanabe, N. Sugimoto, S. Ito, T. Hanada, J. Luminescence **87–89**, 670 (2000).
[7] Y. Ohishi, A. Mori, M. Yamada, H. Ono, Y. Nishida, K. Oikawa, Opt. Lett**. 23**, 274 (1998).
[8] N. Sugimoto, Y. Kuroiwa, K. Ochiai, Y. Fukasawa, S. Ito, S. Tanabe, T. Hanada, in: Opt. Amplifiers and Their Applications, 2000, paper PDP3.
[9] S. W. Harun, N. Tamchek, S. Shahi, H. Ahmad**,** Progress In Electromagnetic Research C **6**, 1 (2009).
[10] W. L. Barnes, R. I. Laming, E. J. Tarbox, P. R. Mokel, IEEE J. Quant. Electron. **274**, 1004 (1991).
[11] E. Snokes, G. N. van den Hoven, A. Polman, J. Opt. Soc. Amer. **B 12**, 1468 (1995).
[12] H. Hayashi, N. Sugimoto, S. Tanabe, Optical Fiber Technology **12**, 282 (2006).
[13] E. Desurvire, Erbium-doped fiber amplifiers: principles and applications, John Wiley & Sons, New York, 1994.

_____
*Corresponding author: swharun@um.edu.my